

# Effective dynamics of the Schwarzschild black hole interior with inverse triad corrections

Hugo A. Morales-Técutl,<sup>1,2,\*</sup> Saeed Rastgoo,<sup>3,1,†</sup> and Juan C. Ruelas<sup>1,‡</sup>

<sup>1</sup>*Departamento de Física, Universidad Autónoma Metropolitana - Iztapalapa  
San Rafael Atlixco 186, Ciudad de Mexico 09340, Mexico*

<sup>2</sup>*Departamento de Física, Escuela Superior de Física  
y Matemáticas del Instituto Politécnico Nacional  
Unidad Adolfo López Mateos, Edificio 9, 07738 Ciudad de México, Mexico*

<sup>3</sup>*School of Sciences and Engineering  
Monterrey Institute of Technology (ITESM), Campus León  
Av. Eugenio Garza Sada, León, Guanajuato 37190, Mexico*

(Dated: June 21, 2022)

We study the interior of the Schwarzschild black hole in the presence of further inverse triad quantum corrections, using loop quantum gravity techniques. Although this model has been studied using loop quantization before, so far, inverse triad corrections have been neglected, mostly to simplify the analysis. Due to the noncompact spatial topology of the model, it is customary to introduce a fiducial cell, to make it possible to define the symplectic structure, but one should be careful so that the physical implications become independent of such fiducial structures. However, this seems to become a hard problem when further triad corrections are present. In this work, we introduce a systematic way to incorporate the inverse triad corrections in the Hamiltonian of the system. The form of the corrections in the present model is related to the way two certain parameters  $\delta_b, \delta_c$  enter the Thiemann's formula. These parameters, in turn, depend on the ratio of the minimum area gap  $\Delta$  to the classical Schwarzschild radius  $r_0$ , or to the height,  $L_0$ , of the fiduciary cell. To deal with the dependence of physical results on  $L_0$ , we consider three possibilities for the parameters: (i)  $\delta_b = \frac{\sqrt{\Delta}}{r_0}$ ,  $\delta_c = \frac{\sqrt{\Delta}}{L_0}$ , (ii)  $\delta_b = \frac{\sqrt{\Delta}}{L_0}$ ,  $\delta_c = \frac{\sqrt{\Delta}}{r_0}$ , and (iii)  $\delta_b = \frac{L_0}{\sqrt{\Delta}}$  and  $\delta_c = \frac{r_0}{\sqrt{\Delta}}$ . Our analysis shows that only (iii), which is different from the sector without inverse triads, leads to physically acceptable results. Furthermore, we retain previous important results such as singularity resolution and black-to-white hole bounce, but with a different value for the minimum radius at bounce, and the mass of the white hole. Finally we discuss how our proposal might be generalized to other models.

\* hugo@xanum.uam.mx

† saeed.rastgoo@tec.mx

‡ j.carlos.ruelas.v@gmail.com

## I. INTRODUCTION

As one of the most fascinating predictions of general relativity, black holes have been the subject of much analysis and explorations. Particularly their interior, and the singularity located there, has been studied in classical, quantum and semiclassical regimes. The mainstream hope and philosophy, is that the classical singularity will be resolved and replaced by a quantum region. However, there are still many open issues to be answered in a satisfactory way. Within loop quantum gravity (LQG) [1, 2], there have been numerous works about quantum black holes and their singularity resolution in both mini- and midi-superspace models, to mention a few [3–14]. One of the most studied models in this context is the Schwarzschild black hole which interior corresponds to a Kantowski-Sachs model, a system with finite degrees of freedom, and hence a mini-superspace, with a singularity at the heart of it [4, 15]. One of the approaches to quantize this model, inspired by LQG, is polymer quantization [16–19], a technique also used in loop quantum cosmology (LQC) [20–22]. In this quantization the classical canonical algebra is represented in a way that is unitarily inequivalent to the usual Schrödinger representation even at the kinematical level. The root of this inequivalency is the choice of topology and the form of the inner product of this representation, which renders some of the operators discontinuous in their parameters, resulting in the representation not being weakly continuous. On the other hand, unitary equivalency of a representation to the Schrödinger one is guaranteed by the Stone-von Neumann theorem iff all of its premises, including weak continuity of the representation, are satisfied, and the polymer representation does not. This inequivalency translates into new results that are different from the usual quantization of the system, one of them being the resolution of the singularity of the Kantowski-Sachs model. These results however, are accompanied by some issues that we briefly discuss in what follows.

In one of the earliest attempts in this approach [3], the authors showed that the singularity can be avoided in the quantum regime, but one of the important issues was the dependence of results on auxiliary parameters that define the size of the fiducial cell. The introduction of this fiducial cell, in this case a cylindrical one with topology  $\mathcal{I} \times \mathbb{S}^2$  and volume  $V_0 = a_0 L_0$ , where  $a_0$  is the area of the 2-sphere  $\mathbb{S}^2$  and  $L_0$  is the cylinder’s height, is necessary to avoid the divergence of some of the spatial integrals in homogenous models with some non-compact directions. Particularly it is important to be able to define the symplectic structure. Given that the physical results should not depend on these auxiliary parameters, a new proposal, motivated by the “improved quantization” in LQC [23], was put forward that avoided this dependence and yielded bounded expansion and shear scalars [4]. However, this method also leads to some undesired modified behavior at the horizon due to quantum gravitational effects in vacuum, that are manifestation of the coordinate singularity there. There are also some other recent works that take a bit of a different approach to the problem by looking for an effective metric [24, 25].

In a recent work, [6], a new method is proposed, with a key modification to the quantization by choosing to fix  $a_0 := 4\pi r_0^2$  by a physical scale  $r_0$ . This physical  $r_0$  permits one to define a Hamiltonian formulation, and in this way is different in nature from the auxiliary scale  $L_0$ , which is needed to fix the fiducial cell size to be able to define the symplectic structure. Thus while  $r_0$  will be present in physical results in both the classical and quantum theories, these theories should be independent of  $L_0$ . The proposal in [6], leads to results that are independent of the auxiliary parameters, and while the theory predicts that the singularity is resolved in the quantum gravity regime, no large quantum gravitational effects

appear at low curvatures near the horizon as it should be the case.

It is worth noting that the anisotropic models suffered from an issue: since these models resolve the singularity, they predicted a “bounce” from a black hole to a white hole, with the mass  $M_W$  of the resultant white hole not matching with that of the original black hole  $M_B \neq M_W$ , but rather  $M_W \propto M_B^4$ . Recent work presented some proposals to deal with it [26] and a different approach was developed in [27, 28] by encompassing the interior region containing the classical singularity with the exterior asymptotic one, which, in the large mass limit, makes the masses of the white and black holes take the same value.

All previous works on black holes ignore some of the further quantum corrections, known as the inverse triad corrections, to simplify the problem. However, they are important especially at highly quantum regimes and a more complete quantum gravitational analysis of this model should take them into account. In this work we first use a path integral in phase space including inverse triad quantum corrections. These corrections are known to produce severe issues in non compact cosmological models, among them the dependence of the physical quantities on the auxiliary parameters or their rescaling. We put forward two proposals that, in the case of Schwarzschild black hole, yield a physical description with no reference to fiducial parameters. Finally, we study how these proposals modify the “minimum radius at the bounce”.

The structure of this paper is as follows: In section II, we present the background, the relation between the Schwarzschild interior and the Kantowski-Sachs model, and their classical Hamiltonian analysis. In section III, we briefly review how the quantum Hamiltonian constraint is defined. In section IV, the path integral analysis is presented and it is shown how a systematic effective Hamiltonian constraint can be derived from the quantum Hamiltonian, including inverse triad corrections. Section V is dedicated to presenting some of the important issues that are raised by the presence of the new corrections, and recognizing the root of these issues. In section VI, we present two proposals to deal with the aforementioned issues, and also show their effect upon some physical quantities. Finally, in section VII, we conclude the paper by presenting a summary and a discussion about the results.

## II. BACKGROUND AND THE CLASSICAL THEORY

For Schwarzschild black hole the spacetime metric

$$ds^2 = - \left(1 - \frac{2GM}{r}\right) dt^2 + \left(1 - \frac{2GM}{r}\right)^{-1} dr^2 + r^2 (d\theta^2 + \sin^2 \theta d\phi^2) \quad (2.1)$$

where  $M$  is the mass of the black hole, the timelike and spacelike curves switch their causal nature into each other for observers that cross the event horizon. Hence one has for the interior region

$$ds^2 = - \left(\frac{2GM}{t} - 1\right)^{-1} dt^2 + \left(\frac{2GM}{t} - 1\right) dr^2 + t^2 (d\theta^2 + \sin^2 \theta d\phi^2), \quad (2.2)$$

with  $t \in (0, 2GM)$  and  $r \in (-\infty, \infty)$ . This metric is a special case of a Kantowski-Sachs cosmological spacetime that is given by the metric

$$ds^2 = -d\tau^2 + A^2(\tau)dr^2 + B^2(\tau) (d\theta^2 + \sin^2 \theta d\phi^2). \quad (2.3)$$

The coordinates in which (2.3) is written are Gaussian normal coordinates adapted to the comoving observers, *i.e.*, the time coordinate curves are the worldlines of the free falling objects (*e.g.* stars) that are at rest with respect to such observers, and are parametrized by their proper time  $\tau$ . The metric (2.2) can be seen to be derived from (2.3) by the transformation

$$d\tau^2 = \left( \frac{2GM}{t} - 1 \right)^{-1} dt^2. \quad (2.4)$$

Choosing positive root of the above, we get

$$\tau = -\sqrt{t(2GM - t)} - GM \tan^{-1} \left( \frac{t - GM}{\sqrt{t(2GM - t)}} \right) + \frac{GM\pi}{2}, \quad (2.5)$$

where the last term in the right hand side is the integration constant and it is chosen such that  $\tau \rightarrow 0$  for  $t \rightarrow 0$  (at singularity), and  $\tau \rightarrow GM\pi$  for  $t \rightarrow 2GM$  (at the horizon), hence  $\tau \in (0, GM\pi)$ . Then  $\tau$  is a monotonic function of  $t$ . Written in Gaussian normal coordinates  $(\tau, r, \theta, \phi)$ , the Schwarzschild metric takes the form (2.3), with  $A^2(\tau) = \frac{2GM}{t(\tau)} - 1$  and  $B^2(\tau) = \tau^2$ .

The Kantowski-Sachs metric (2.3) in general and the Schwarzschild interior (2.2) in particular, represent a spacetime with spatial homogeneous but anisotropic foliations; one can consider  $A(\tau)$  and  $B(\tau)$  as two distinct scale factors that affect the radial and angular parts of the metric separately. Thus the interior region is a model with no local degrees of freedom, *i.e.*, it can be described as a mechanical system with a finite number of configuration variables. In gravitational language, this corresponds to a mini-superspace model. From the computational point of view, this is an important property that is exploited in quantizing the Schwarzschild interior as we will see.

It also can be seen from the metric (2.3) and (2.2), that the spacetime is foliated such that the spatial hypersurfaces have topology  $\mathbb{R} \times \mathbb{S}^2$ , and the symmetry group is the Kantowski-Sachs isometry group  $\mathbb{R} \times SO(3)$ . The aforementioned topology of the model means that there exists one noncompact direction,  $r \in \mathbb{R}$  in space. Thus in order to be able to compute quantities that involve integrals over space, particularly the symplectic structure  $\int_{\mathbb{R} \times \mathbb{S}^2} d^3x dq \wedge dp$ , one needs to choose a finite fiducial volume over which these integrals are calculated, otherwise the integrals will diverge. This is a common practice in the study of homogeneous minisuperspace models, which here, is done by introducing an auxiliary length  $L_0$  to restrict the noncompact direction to an interval  $r \in \mathcal{I} = [0, L_0]$ . The volume of the fiducial cylindrical cell in this case is  $V_0 = a_0 L_0$ , where  $a_0$  is the area of the 2-sphere  $\mathbb{S}^2$  in  $\mathcal{I} \times \mathbb{S}^2$ . Now, for the area  $a_0$ , there are at least two choices: One can use leave it as an auxiliary variable, or fix it using a physical scale. In any case, the final physical results should not depend on the choice of auxiliary parameters. In a recent work [6], a choice has been put forward, in which the  $\mathbb{S}^2$  area of the fiducial volume is fixed to be  $a_0 := 4\pi r_0^2$  where  $r_0$  is a physical scale that is identified with the Schwarzschild radius. This choice can be considered as a boundary condition which ensures that the classical limit becomes the classical Schwarzschild solution with radius  $r_0$ . Using this choice, the volume of the cylindrical fiducial cell becomes  $V_0 = 4\pi r_0^2 L_0$ , and the associated fiducial metric is denoted by  ${}^0q_{ab}$ . Using a physical scale for  $a_0$ , instead of an auxiliary nonphysical one, seems to be a key ingredient that fixes some of the issues with previous attempts at loop quantization of the interior of Schwarzschild black hole, and here we follow this choice.

The starting point of the Hamiltonian analysis in this approach is to write down the classical configuration variable, the  $su(2)$  Ashtekar-Barbero connection  $A_a^i$ , and its conjugate

momentum, the desitized triad  $E_i^a$ , in the relevant coordinate basis. Given the symmetries of this spacetime and after imposing the Gauss constraint, these variables take the form [3, 6]

$$A_a^i \tau_i dx^a = \bar{c} \tau_3 dr + \bar{b} r_0 \tau_2 d\theta - \bar{b} r_0 \tau_1 \sin \theta d\phi + \tau_3 \cos \theta d\phi, \quad (2.6)$$

$$E_i^a \tau^i \frac{\partial}{\partial x^a} = \bar{p}_c r_0^2 \tau_3 \sin \theta \frac{\partial}{\partial r} + \bar{p}_b r_0 \tau_2 \sin \theta \frac{\partial}{\partial \theta} - \bar{p}_b r_0 \tau_1 \frac{\partial}{\partial \phi}, \quad (2.7)$$

where  $\bar{b}$ ,  $\bar{c}$ ,  $\bar{p}_b$  and  $\bar{p}_c$  are functions that only depend on time  $t$ , and  $\tau_i = -i\sigma_i/2$  are a  $su(2)$  basis with  $\sigma_i$  being the Pauli matrices.  $r_0 = 2GM$  is the Schwarzschild radius. In these variables the Schwarzschild interior metric becomes

$$ds^2 = -N^2 dt^2 + \frac{\bar{p}_b^2}{|\bar{p}_c|} dr^2 + |\bar{p}_c| r_0^2 (d\theta^2 + \sin^2 \theta d\phi^2). \quad (2.8)$$

The fiducial connection and triad related to (2.6) and (2.7) are

$${}^0 A_a^i \tau_i dx^a = \tau_3 dr + r_0 \tau_2 d\theta - r_0 \tau_1 \sin \theta d\phi + \tau_3 \cos \theta d\phi, \quad (2.9)$$

$${}^0 E_i^a \tau^i \frac{\partial}{\partial x^a} = r_0^2 \tau_3 \sin \theta \frac{\partial}{\partial r} + r_0 \tau_2 \sin \theta \frac{\partial}{\partial \theta} - \bar{p}_b \tau_1 \frac{\partial}{\partial \phi}. \quad (2.10)$$

and the fiducial metric is written as

$$ds_0^2 := dr^2 + r_0^2 (d\theta^2 + \sin^2 \theta d\phi^2), \quad (2.11)$$

where  $r$  takes values within the interval  $\mathcal{I} = [0, L_0]$ .

Now, the symplectic structure can be computed by performing an integration over the fiducial volume as

$$\begin{aligned} \Xi &= \frac{1}{8\pi G\gamma} \int_{\mathcal{I} \times \mathbb{S}^2} d^3x \quad dA_a^i \wedge dE_i^a \\ &= \frac{L_0 r_0^2}{2G\gamma} (d\bar{c} \wedge d\bar{p}_c + 2d\bar{b} \wedge d\bar{p}_b), \end{aligned} \quad (2.12)$$

where  $\gamma$  is the Barbero-Immirzi parameter [1]. Clearly, in these variables, the symplectic structure and thus the Poisson algebra depends on  $L_0$ . To remove this dependency, it is customary to redefine the variables in the following way

$$c = L_0 \bar{c}, \quad p_c = r_0^2 \bar{p}_c \quad b = r_0 \bar{b} \quad p_b = r_0 L_0 \bar{p}_b. \quad (2.13)$$

As a result the Poisson algebra between these redefined variables is independent of the auxiliary variable  $L_0$ ,

$$\{c, p_c\} = 2G\gamma, \quad \{b, p_b\} = G\gamma, \quad (2.14)$$

and the physical metric takes the form

$$ds^2 = -N^2 dt^2 + \frac{p_b^2}{L_0^2 |p_c|} dx^2 + |p_c| (d\theta^2 + \sin^2 \theta d\phi^2). \quad (2.15)$$

By comparing this metric with (2.2), and assuming we are working in Schwarzschild coordinates, we can see that

$$\frac{p_b^2}{L_0^2 |p_c|} = \left( \frac{2GM}{t} - 1 \right), \quad |p_c| = t^2. \quad (2.16)$$

This means that

$$p_b = 0, \quad p_c = 4G^2 M^2, \quad \text{On the horizon } t = 2GM \ (\tau = GM\pi), \quad (2.17)$$

$$p_b \rightarrow 0, \quad p_c \rightarrow 0, \quad \text{At singularity } t = 0 \ (\tau = 0), \quad (2.18)$$

where  $t$  is the time in Schwarzschild coordinates, and we have used the Schwarzschild lapse  $N = \left(\frac{2GM}{t} - 1\right)^{-\frac{1}{2}}$  to find the corresponding proper times  $\tau = \int N dt \in (0, GM\pi)$ .

Although the redefinitions (2.13), transform the metric such that it remains invariant under coordinate rescaling  $r \rightarrow \xi r$ , there still exists a freedom in rescaling the length of the interval  $\mathcal{I}$  itself by  $L_0 \rightarrow \xi L_0$ . This freedom manifests itself in transformation of the canonical variables in the following way

$$c \rightarrow c' = \xi c \quad p_c \rightarrow p'_c = p_c, \quad (2.19)$$

$$b \rightarrow b' = b \quad p_b \rightarrow p'_b = \xi p_b. \quad (2.20)$$

Note that here [6], since  $r_0$  is chosen to be a physical scale, not an auxiliary one, there is no freedom associated with its rescaling, unlike the case in [3].

### III. THE QUANTUM HAMILTONIAN CONSTRAINT

The next step is to find the classical Hamiltonian in loop variables, and then representing it as an operator on a suitable kinematical Hilbert space. We only briefly go over this, details can be found in previous works [3, 7]. Since in this model, the diffeomorphism constraint is trivially satisfied, after imposing the Gauss constraint, one is left only with the classical Hamiltonian constraint

$$C = - \int \frac{d^3x}{\sqrt{|\det E|}} \epsilon_{ijk} E^{ai} E^{bj} \left( \frac{1}{\gamma^2} {}^0F_{ab}^k - \Omega_{ab}^k \right). \quad (3.1)$$

Here the integral is over the fiducial volume, and  $\Omega_{ab}^k$  and  ${}^0F_{ab}^k$  are the curvatures of the spin connection  $\Gamma_a^i$ , and the extrinsic curvature  $K_a^i = \frac{1}{\gamma} (A_a^i - \Gamma_a^i)$ , respectively. Since in loop quantum gravity the configuration variables are holonomies, not the connections themselves, these curvatures should be written in terms of them. In general, the holonomy of a connection  $A_a^i$  over edge  $e$  is the path ordered exponential

$$h_e[A] = \mathcal{P}\exp \left( \int_e A_a^i \tau_i dx^a \right). \quad (3.2)$$

In case of the present model, there are two types of holonomies: the one that is integrated over a path (or edge)  $\lambda$ , in the  $r$  direction,

$$h_r^{(\lambda)} = \cos \left( \frac{\lambda c}{2} \right) + 2\tau_3 \sin \left( \frac{\lambda c}{2} \right) \quad (3.3)$$

and the ones that are over edges  $\mu$ , in  $\theta$  and  $\phi$  directions,

$$h_\theta^{(\mu)} = \cos \left( \frac{\mu b}{2} \right) + 2\tau_2 \sin \left( \frac{\mu b}{2} \right), \quad (3.4)$$

$$h_\phi^{(\mu)} = \cos \left( \frac{\mu b}{2} \right) - 2\tau_1 \sin \left( \frac{\mu b}{2} \right). \quad (3.5)$$

To find the curvature, one considers loops in  $r - \theta$ ,  $r - \phi$  and  $\theta - \phi$  planes, such that the edges along the  $r$  direction in  $\mathbb{R}$  have a length  $\delta_c \ell_c$  where  $\ell_c = L_0$ , and the edges along the longitude and the equator of  $\mathbb{S}^2$  have length  $\delta_b \ell_b$  where  $\ell_b = r_0$ . Then the curvature  ${}^0F_{ab}^k$  can be computed in terms of holonomies as

$${}^0F_{ab}^k = -2 \lim_{\text{Ar}\square \rightarrow 0} \text{Tr} \left( \frac{h_{\square ij}^{(\delta_{(i)}, \delta_{(j)})} - 1}{\delta_{(i)} \ell_{(i)} \delta_{(j)} \ell_{(j)}} \right) {}^0E_a^i {}^0E_b^j \tau^k, \quad (3.6)$$

in which

$$h_{\square ij}^{(\delta_{(i)}, \delta_{(j)})} = h_i^{(\delta_{(i)})} h_j^{(\delta_{(j)})} \left( h_i^{(\delta_{(i)})} \right)^{-1} \left( h_j^{(\delta_{(j)})} \right)^{-1}. \quad (3.7)$$

Here  $\delta_{(i)}$  correspond to  $\delta_b$  or  $\delta_c$ ,  $\ell_{(i)}$  correspond to  $\ell_{(b)}$  or  $\ell_{(c)}$ ,  $\square_{ij}$  is the loop with edges  $i, j$ , and  $\text{Ar}\square$  is the area of the loop over which the curvature is being computed, and its limit to zero has been taken. Note, however, that in the quantum regime, due to the discreteness of the area, the loops can only be shrunk to a minimum value of  $\Delta = \zeta \ell_{\text{Pl}}^2$  with  $\zeta \approx \mathcal{O}(1)$  [3]. It turns out that by following [6], one gets

$$\delta_b = \frac{\sqrt{\Delta}}{r_0}, \quad \delta_c = \frac{\sqrt{\Delta}}{L_0}. \quad (3.8)$$

As for the factor outside the parenthesis in (3.1), which contains the inverse triad, we rewrite it using Thiemann's formula

$$\frac{\epsilon_{ijk}}{\sqrt{|\det E|}} E^{aj} E^{bk} = \sum_k \frac{{}^0\epsilon^{abc} {}^0E_c^k}{2\pi\gamma G \delta_{(k)} \ell_{(k)}} \text{Tr} \left( h_k^{(\delta_{(k)})} \left\{ \left( h_k^{(\delta_{(k)})} \right)^{-1}, V \right\} \tau_i \right), \quad (3.9)$$

in which  $V$ , the physical volume of the fiducial cell, is

$$V = \int d^3x \sqrt{\det q} = 4\pi |p_b| |p_c|^{1/2}. \quad (3.10)$$

Using (3.6), (3.9) and (3.10) in (3.1), we get

$$\begin{aligned} C^{(\delta_b, \delta_c)} = & -\frac{2}{\gamma^3 G \delta_b^2 \delta_c} \left[ 2\gamma^2 \delta_b^2 \text{Tr} \left( \tau_3 h_x^{(\delta_c)} \left\{ \left( h_x^{(\delta_c)} \right)^{-1}, V \right\} \right) \right. \\ & \left. + \sum_{ijk} \epsilon^{ijk} \text{Tr} \left( h_{\square ij}^{(\delta_{(i)}, \delta_{(j)})} h_k^{(\delta_{(k)})} \left\{ \left( h_k^{(\delta_{(k)})} \right)^{-1}, V \right\} \right) \right]. \end{aligned} \quad (3.11)$$

To construct the kinematical Hilbert space on which this Hamiltonian constraint is to be represented, one notes that the algebra generated by the holonomies (3.3)-(3.5), is the algebra of the almost periodic functions of the form  $\exp(i(\mu b + \lambda c)/2)$ . This algebra (for just  $b$  or  $c$ ) is isomorphic to the algebra of the continuous functions on the Bohr compactification of  $\mathbb{R}$ . Thus the kinematical Hilbert space corresponding to this space of configurations turns out to be the Cauchy completion of the space of square integrable functions over the Bohr compactified  $\mathbb{R}^2$ , together with its associated Haar measure  $\mathcal{H}_{\text{kin}} = L^2(\mathbb{R}_{\text{Bohr}}^2, d^2\mu_{\text{Bohr}})$ . The basis states of this space satisfy the relation

$$\langle \mu', \lambda' | \mu, \lambda \rangle = \delta_{\mu, \mu'} \delta_{\lambda, \lambda'}, \quad (3.12)$$

where on the right hand side we have Kronecker deltas instead of Dirac deltas. On this space, in the momentum basis, the basic variables are represented as

$$\widehat{e^{\frac{1}{2}i\delta_b b}}|\mu, \lambda\rangle = |\mu + \delta_b, \lambda\rangle, \quad \widehat{e^{\frac{1}{2}i\delta_c c}}|\mu, \lambda\rangle = |\mu, \lambda + \delta_c\rangle, \quad (3.13)$$

$$\hat{p}_b|\mu, \lambda\rangle = \frac{\gamma\ell_{\text{Pl}}^2}{2}\mu|\mu, \lambda\rangle, \quad \hat{p}_c|\mu, \lambda\rangle = \gamma\ell_{\text{Pl}}^2\lambda|\mu, \lambda\rangle. \quad (3.14)$$

This is the quantum mechanical polymer representation corresponding to the original classical variables, which is unitarily inequivalent to the Schrödinger representation, due to some of the operators not being weakly continuous in their parameters, and hence the representation not satisfying the weak continuity premise of the Stone-von Neumann theorem. Due to the lack of weak continuity, the operators  $\hat{b}$  and  $\hat{c}$  are not well-defined on  $\mathcal{H}_{\text{kin}}$ , and thus their corresponding infinitesimal transformations do not exist. The theory, thus, only contains their corresponding finite transformations due to the action of  $\widehat{e^{\frac{1}{2}i\delta_b b}}$  and  $\widehat{e^{\frac{1}{2}i\delta_c c}}$ , which are not to be considered as the literal exponentiation of  $\hat{b}$  and  $\hat{c}$ . This finite transformation is evident from (3.13). These result in  $p_b$  and  $p_c$  (components of the triad  $E_i^a$ ) being discrete in the sense that they can only change by a finite minimum value. This, in principle, is how this approach yields the quantization and discreteness of the geometry.

Using the above consideration, the Hamiltonian constraint (3.11), is represented as

$$\begin{aligned} \hat{C}^{(\delta_b, \delta_c)} = & \frac{32i}{\gamma^3 \delta_b^2 \delta_c \ell_{\text{Pl}}^2} \left\{ \left[ \sin\left(\frac{\delta_b b}{2}\right) \cos\left(\frac{\delta_b b}{2}\right) \sin\left(\frac{\delta_c c}{2}\right) \cos\left(\frac{\delta_c c}{2}\right) \right] \right. \\ & \times \left[ \sin\left(\frac{\delta_b b}{2}\right) \hat{V} \cos\left(\frac{\delta_b b}{2}\right) - \cos\left(\frac{\delta_b b}{2}\right) \hat{V} \sin\left(\frac{\delta_b b}{2}\right) \right] \\ & + \frac{1}{2} \left[ \sin^2\left(\frac{\delta_b b}{2}\right) \cos^2\left(\frac{\delta_b b}{2}\right) + \frac{1}{4} \gamma^2 \delta_b^2 \right] \\ & \left. \times \left[ \sin\left(\frac{\delta_c c}{2}\right) \hat{V} \cos\left(\frac{\delta_c c}{2}\right) - \cos\left(\frac{\delta_c c}{2}\right) \hat{V} \sin\left(\frac{\delta_c c}{2}\right) \right] \right\}, \quad (3.15) \end{aligned}$$

where  $\hat{V}$  is the quantum volume operator, which is the representation of the classical volume (3.10), on  $\mathcal{H}_{\text{kin}}$ . To make a well defined constraint operator we introduce its symmetric version  $\hat{C}_S^{(\delta_b, \delta_c)} = \frac{1}{2} \left( \hat{C}^{(\delta_b, \delta_c)} + \hat{C}^{(\delta_b, \delta_c)\dagger} \right)$ .

#### IV. PATH INTEGRAL ANALYSIS: EFFECTIVE HAMILTONIAN AND NEW FEATURES

To find the effective version of the constraint we employ path integration. For standard mechanical systems path integrals yield expressions for the matrix elements of the evolution operators. The original derivation by Feynman involved the canonical theory expressing the evolution by composing  $\mathcal{N}$  infinitesimal ones and inserting complete basis between these. Such discrete time path integral gets replaced by the continuum one in the limit  $\mathcal{N} \rightarrow \infty$ . For gravitational models we have two different, but equivalent, routes to follow [29] (See [17, 19] for the case of non gravitational models): the use of a relational or deparametrized time scheme in which a matter degree of freedom is used as a clock, or else consider a timeless scheme that may include matter. In the latter case there is no evolution operator



but a constraint and its solutions, and we consider this scheme next. The aim is to construct a path integral expression for the so called “extraction amplitude” [29]

$$A(\mu_f, \lambda_f; \mu_i, \lambda_i) = \int d\alpha \left\langle \mu_f, \lambda_f \left| e^{-i\alpha \hat{C}_S^{(\delta_b, \delta_c)}} \right| \mu_i, \lambda_i \right\rangle, \quad (4.1)$$

which is a Green function for the transformation between kinematical and physical states, those that are annihilated by the quantum Hamiltonian constraint,

$$|\Psi_{\text{phys}}\rangle = \int d\alpha e^{-i\alpha \hat{C}_S^{(\delta_b, \delta_c)}} |\Psi_{\text{kin}}\rangle \quad (4.2)$$

with  $|\Psi_{\text{kin}}\rangle \in \mathcal{H}_{\text{kin}}$ , namely

$$\Psi_{\text{phys}}(\mu, \lambda) = \sum_{\lambda', \mu'} A(\mu, \lambda; \mu', \lambda') \Psi_{\text{kin}}(\mu', \lambda'). \quad (4.3)$$

To find the path integral representation of this Green function, as usual, we employ the “time slicing” method [29], by dividing the fictitious unit time interval into  $\mathcal{N}$  sub-intervals each with length  $\epsilon = \frac{1}{\mathcal{N}}$  such that

$$A(\mu_f, \lambda_f, \mu, \lambda_i) = \left\langle \mu_f, \lambda_f \left| \underbrace{e^{-i\epsilon \hat{C}_S^{(\delta_b, \delta_c)}} \dots e^{-i\epsilon \hat{C}_S^{(\delta_b, \delta_c)}}}_{\mathcal{N} \text{ times}} \right| \mu_i, \lambda_i \right\rangle. \quad (4.4)$$

By inserting  $\hat{\mathbb{I}} = \sum_{(\mu, \lambda) \in \Gamma} |\mu, \lambda\rangle \langle \mu, \lambda|$ , between the exponentials above, the amplitude is written as

$$A(\mu_f, \lambda_f, \mu, \lambda_i) = \prod_{n=1}^{\mathcal{N}} \sum_{\mu_n, \lambda_n \in \gamma} \left\langle \mu_n, \lambda_n \left| e^{-i\epsilon \hat{C}_S^{(\delta_b, \delta_c)}} \right| \mu_{n-1}, \lambda_{n-1} \right\rangle, \quad (4.5)$$

where  $\mu_{\mathcal{N}}, \lambda_{\mathcal{N}}, \mu_0, \lambda_0$  correspond to  $\mu_f, \lambda_f, \mu_i, \lambda_i$  respectively. Each “short-time” amplitude can be expanded up to first order in  $\epsilon$  as

$$\begin{aligned} \left\langle \mu_n, \lambda_n \left| e^{-i\epsilon \hat{C}_S^{(\delta_b, \delta_c)}} \right| \mu_{n-1}, \lambda_{n-1} \right\rangle &= \delta_{\mu_n, \mu_{n-1}} \delta_{\lambda_n, \lambda_{n-1}} - i\epsilon \left\langle \mu_n, \lambda_n \left| \hat{C}_S^{(\delta_b, \delta_c)} \right| \mu_{n-1}, \lambda_{n-1} \right\rangle + \mathcal{O}(\epsilon^2), \\ &= \left( \frac{1}{2\pi} \right)^2 \int_{-\pi/p_b^0}^{\pi/p_b^0} db_n \int_{-\pi/p_c^0}^{\pi/p_c^0} dc_n e^{-ib_n(p_n^b - p_{n-1}^b) - ic_n(p_n^c - p_{n-1}^c)} \\ &\quad - i\epsilon \left\langle \mu_n, \lambda_n \left| \hat{C}_S^{(\delta_b, \delta_c)} \right| \mu_{n-1}, \lambda_{n-1} \right\rangle + \mathcal{O}(\epsilon^2), \end{aligned} \quad (4.6)$$

where we have used  $p_n^b = \frac{1}{2}\gamma\ell_{\text{Pl}}^2\mu_n$  and  $p_n^c = \gamma\ell_{\text{Pl}}^2\lambda_n$ .

To proceed, we need to compute the matrix element of the quantum Hamiltonian constraint  $\hat{C}_S^{(\delta_b, \delta_c)}$ . This turns out to be

$$\begin{aligned} \left\langle \mu', \lambda' \left| \hat{C}_S^{(\delta_b, \delta_c)} \right| \mu, \lambda \right\rangle &= -\frac{1}{\gamma^3 \delta_b^2 \delta_c \ell_{\text{Pl}}^2} [(V_{\mu+\delta_b, \lambda} - V_{\mu-\delta_b, \lambda}) \\ &\quad \times (\delta_{\mu', \mu+2\delta_b} - \delta_{\mu', \mu-2\delta_b}) (\delta_{\lambda', \lambda+2\delta_c} - \delta_{\lambda', \lambda-2\delta_c}) \\ &\quad + \frac{1}{2} (V_{\mu, \lambda+\delta_c} - V_{\mu, \lambda-\delta_c}) \delta_{\lambda', \lambda} \\ &\quad \times (\delta_{\mu', \mu+4\delta_b} - 2(1 + 2\delta_b^2 \gamma^2) \delta_{\mu', \mu} + \delta_{\mu', \mu-4\delta_b})], \end{aligned} \quad (4.7)$$

where  $V_{\mu,\lambda}$  is the eigenvalue of the quantum volume operator  $\hat{V}$  in this basis. It is computed by using (3.14) to represent the classical volume (3.10), and then acting it on this basis,

$$\hat{V}|\mu, \lambda\rangle = V_{\mu,\lambda}|\mu, \lambda\rangle = 2\pi\gamma^{3/2}\ell_{\text{Pl}}^3|\mu||\lambda|^{1/2}|\mu, \lambda\rangle. \quad (4.8)$$

Using this, the matrix element (4.7) becomes

$$\left\langle \mu_n, \lambda_n \left| \hat{C}_S^{(\delta_b, \delta_c)} \right| \mu_{n-1}, \lambda_{n-1} \right\rangle = \frac{2}{\gamma^3 \ell_{\text{Pl}}^2} \left( \frac{1}{2\pi} \right)^2 \int_{-\pi/p_b^0}^{\pi/p_b^0} db_n \int_{-\pi/p_c^0}^{\pi/p_c^0} dc_n \left\{ e^{-ib_n(p_n^b - p_{n-1}^b) - ic_n(p_n^c - p_{n-1}^c)} \right. \quad (4.9)$$

$$\left. \times \left[ 2V_1^n \frac{\sin(\delta_b b_n)}{\delta_b} \frac{\sin(\delta_c c_n)}{\delta_c} + V_2^n \left( \frac{\sin^2(\delta_b b_n)}{\delta_b^2} + \gamma^2 \right) \right] \right\}, \quad (4.10)$$

where

$$V_2^n := \begin{cases} \pi\gamma^{3/2}\ell_{\text{Pl}}^3|\mu_n| \frac{(\lambda_n + \delta_c)^{1/2} - (\lambda_n - \delta_c)^{1/2}}{\delta_c} & \lambda_n \geq \delta_c \\ \pi\gamma^{3/2}\ell_{\text{Pl}}^3|\mu_n| \frac{(\lambda_n + \delta_c)^{1/2} - (\delta_c - \lambda_n)^{1/2}}{\delta_c} & |\lambda_n| < \delta_c \\ \pi\gamma^{3/2}\ell_{\text{Pl}}^3|\mu_n| \frac{(-\lambda_n - \delta_c)^{1/2} - (\delta_c - \lambda_n)^{1/2}}{\delta_c} & \lambda_n \leq -\delta_c \end{cases} \quad (4.11)$$

$$= 4\pi\gamma\ell_{\text{Pl}}^2|p_n^b| \frac{\left( \sqrt{|p_n^c + p_c^0|} - \sqrt{|p_n^c - p_c^0|} \right)}{p_c^0},$$

and

$$V_1^n := \begin{cases} \pi\gamma^{3/2}\ell_{\text{Pl}}^3|\lambda_n|^{1/2} & \mu_n \geq \delta_b \\ \pi\gamma^{3/2}\ell_{\text{Pl}}^3|\lambda_n|^{1/2}\mu_n/\delta_b & |\mu_n| < \delta_b \\ -\pi\gamma^{3/2}\ell_{\text{Pl}}^3|\lambda_n|^{1/2} & \mu_n \leq -\delta_b \end{cases} \quad (4.12)$$

$$= 4\pi\gamma\ell_{\text{Pl}}^2|p_n^c|^{\frac{1}{2}} \frac{|p_n^b + p_b^0| - |p_n^b - p_b^0|}{2p_b^0},$$

with

$$p_b^0 := \frac{1}{2}\gamma\ell_{\text{Pl}}^2\delta_b, \quad p_c^0 := \gamma\ell_{\text{Pl}}^2\delta_c. \quad (4.13)$$

Substituting all these back into the short-time amplitude (4.6) yields

$$\begin{aligned} \left\langle \mu_n, \lambda_n \left| e^{-i\epsilon\hat{C}_S^{(\delta_b, \delta_c)}} \right| \mu_{n-1}, \lambda_{n-1} \right\rangle &= \int_{-\pi/p_b^0}^{\pi/p_b^0} db_n \int_{-\pi/p_c^0}^{\pi/p_c^0} dc_n \left\{ e^{-ib_n(p_n^b - p_{n-1}^b) - ic_n(p_n^c - p_{n-1}^c)} \right. \\ &\quad \times \left( 1 - i\epsilon\tilde{C}(p_n^b, p_n^c, b_n, c_n) \right) \left. \right\} + \mathcal{O}(\epsilon^2) \\ &= \int_{-\pi/p_b^0}^{\pi/p_b^0} db_n \int_{-\pi/p_c^0}^{\pi/p_c^0} dc_n \left\{ e^{-ib_n(p_n^b - p_{n-1}^b) - ic_n(p_n^c - p_{n-1}^c) - i\epsilon\tilde{C}(p_n^b, p_n^c, b_n, c_n)} \right\} \\ &\quad + \mathcal{O}(\epsilon^2), \end{aligned} \quad (4.14)$$

where

$$\tilde{C}(p_n^b, p_n^c, b_n, c_n) = \frac{2}{\gamma^3 \ell_{\text{Pl}}^2} \left[ 2V_1^n \frac{\sin(\delta_b b_n)}{\delta_b} \frac{\sin(\delta_c c_n)}{\delta_c} + V_2^n \left( \frac{\sin^2(\delta_b b_n)}{\delta_b^2} + \gamma^2 \right) \right]. \quad (4.15)$$

The amplitude (4.5), is the multiplication of these ‘short-time’ amplitudes,

$$A(\mu_f, \lambda_f, \mu, \lambda_i) = \prod_{n=1}^{\mathcal{N}} \sum_{\mu_n, \lambda_n \in \Gamma} \int_{-\pi/p_b^0}^{\pi/p_b^0} db_n \int_{-\pi/p_c^0}^{\pi/p_c^0} dc_n \left\{ \exp \left( -i \left[ \epsilon \sum_{n=1}^{\mathcal{N}} \frac{b_n (p_n^b - p_{n-1}^b) + c_n (p_n^c - p_{n-1}^c)}{\epsilon} + \epsilon \sum_{n=1}^{\mathcal{N}} \tilde{C}(p_n^b, p_n^c, b_n, c_n) \right] \right) \right\} + \mathcal{O}(\epsilon^2).$$

The first term in the exponential can be written as

$$\sum_{n=1}^{\mathcal{N}} b_n (p_n^b - p_{n-1}^b) + c_n (p_n^c - p_{n-1}^c) = \text{B.T.} - \sum_{n=1}^{\mathcal{N}-1} (b_{n+1} - b_n) p_n^b + (c_{n+1} - c_n) p_n^c, \quad (4.16)$$

where B.T. is the boundary term

$$\text{B.T.} = b_{\mathcal{N}} p_{\mathcal{N}}^b - b_1 p_0^b + c_{\mathcal{N}} p_{\mathcal{N}}^c - c_1 p_0^c. \quad (4.17)$$

Then, the amplitude becomes

$$A(\mu_f, \lambda_f, \mu, \lambda_i) = \prod_{n=1}^{\mathcal{N}} \sum_{\mu_n, \lambda_n \in \Gamma} \int_{-\pi/p_b^0}^{\pi/p_b^0} db_n \int_{-\pi/p_c^0}^{\pi/p_c^0} dc_n \left\{ \exp \left( i \left[ \epsilon \sum_{n=1}^{\mathcal{N}} \frac{b_{n+1} - b_n}{\epsilon} p_n^b + \frac{c_{n+1} - c_n}{\epsilon} p_n^c - \epsilon \sum_{n=1}^{\mathcal{N}} \tilde{C}(p_n^b, p_n^c, b_n, c_n) + \text{B.T.} \right] \right) \right\} + \mathcal{O}(\epsilon^2).$$

Finally taking the limit  $\mathcal{N} \rightarrow \infty$  such that  $\mathcal{N}\epsilon = 1$ , we arrive at

$$A(\mu_f, \lambda_f, \mu, \lambda_i) = \int Db \int Dc \exp \left\{ i \int_{t_i}^{t_f} dt \left[ p_b \dot{b} + p_c \dot{c} - C_{\text{S-eff}}^{(\delta_b, \delta_c)}(p_b(t), p_c(t), b(t), c(t)) \right] + \underbrace{b_f p_f^b - b_i p_i^b + c_f p_f^c - c_i p_i^c}_{\text{B.T.}} \right\} \quad (4.18)$$

where in the limit taken,  $\epsilon \sum_{n=1}^{\mathcal{N}-1} \rightarrow \int dt$ , and  $p_n^c, p_n^b \rightarrow p_c(t), p_b(t)$ , respectively, and

$$\int Db \int Dc = \lim_{\mathcal{N} \rightarrow \infty} \prod_{n=1}^{\mathcal{N}} \sum_{\mu_n, \lambda_n \in \Gamma} \int_{-\pi/p_b^0}^{\pi/p_b^0} db_n \int_{-\pi/p_c^0}^{\pi/p_c^0} dc_n. \quad (4.19)$$

From this, one can read off the effective Hamiltonian constraint from the path integral representation of the kernel as

$$C_{\text{S-eff}}^{(\delta_b, \delta_c)}(p_b, p_c, p_b, p_c) = -\frac{2}{\gamma^3 \ell_{\text{Pl}}^2} \left[ 2V_1(p_b, p_c) \frac{\sin(\delta_b b)}{\delta_b} \frac{\sin(\delta_c c)}{\delta_c} + V_2(p_b, p_c) \left( \frac{\sin^2(\delta_b b)}{\delta_b^2} + \gamma^2 \right) \right]. \quad (4.20)$$

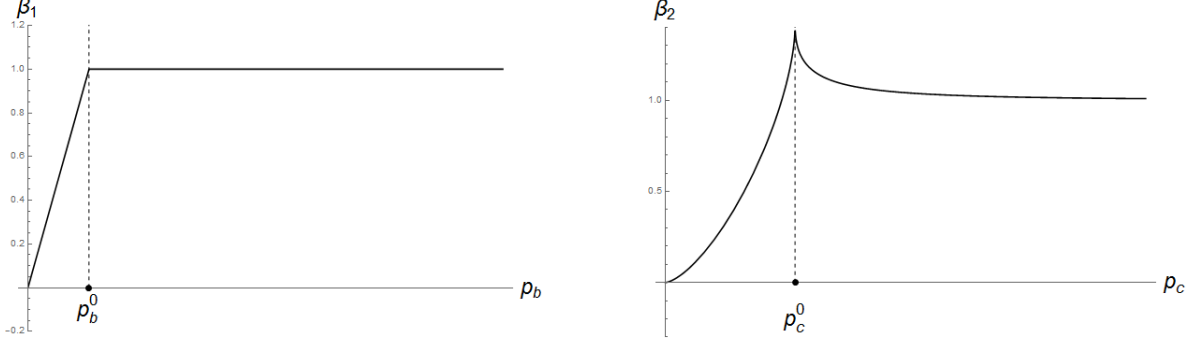


Figure 1. The functions  $\beta_1$  and  $\beta_2$ , with  $p_b = 1 = p_c$ . It is seen that for  $p_b > p_b^0$  and  $p_c \gg p_c^0$ , they behave as  $\beta_1, \beta_2 \rightarrow 1$ .

Here

$$V_1(p_b, p_c) = \lim_{p_n^b, p_n^c \rightarrow p_b(t), p_c(t)} V_1^n = 4\pi\gamma\ell_{\text{Pl}}^2 \beta_1(p_b, p_b^0) |p_c|^{\frac{1}{2}}, \quad (4.21)$$

with

$$\beta_1(p_b, p_b^0) = \frac{|p_b + p_b^0| - |p_b - p_b^0|}{2p_b^0}. \quad (4.22)$$

In the same manner

$$V_2(p_b, p_c) = \lim_{p_n^b, p_n^c \rightarrow p_b(t), p_c(t)} V_2^n = 4\pi\gamma\ell_{\text{Pl}}^2 \beta_2(p_c, p_c^0) \frac{|p_b|}{|p_c|^{\frac{1}{2}}}, \quad (4.23)$$

in which

$$\beta_2(p_c, p_c^0) = |p_c|^{\frac{1}{2}} \frac{\left(\sqrt{|p_c + p_c^0|} - \sqrt{|p_c - p_c^0|}\right)}{p_c^0}. \quad (4.24)$$

With introduction of  $\beta_1$  and  $\beta_2$ , the effective Hamiltonian (4.20) times the lapse function,  $\frac{N}{16\pi G}$ , is written as

$$C_{\text{S-eff}}^{(\delta_b, \delta_c)} = -\frac{N}{2G\gamma^2} \left[ 2\beta_1(p_b, p_b^0) |p_c|^{\frac{1}{2}} \frac{\sin(\delta_b b)}{\delta_b} \frac{\sin(\delta_c c)}{\delta_c} + \beta_2(p_c, p_c^0) \frac{|p_b|}{|p_c|^{\frac{1}{2}}} \left( \frac{\sin^2(\delta_b b)}{\delta_b^2} + \gamma^2 \right) \right]. \quad (4.25)$$

This effective Hamiltonian resembles the ones that have been suggested in previous works, with the important difference of incorporating further inverse triad quantum corrections, encoded in functions  $\beta_1$  and  $\beta_2$ , as can be seen from (4.22) and (4.24). The profile of these functions are plotted in Fig. 1.

For a generic lapse function  $N$ , this effective Hamiltonian leads to the equations of motion,

$\dot{F} = \left\{ F, C_{\text{S-eff}}^{(\delta_b, \delta_c)} \right\}$ , that read

$$\begin{aligned} \dot{b} = & -\frac{1}{2\gamma} \left[ 2\beta_1 (p_b, p_b^0) |p_c|^{\frac{1}{2}} \frac{\sin(\delta_b b)}{\delta_b} \frac{\sin(\delta_c c)}{\delta_c} \{b, N\} \right. \\ & + \beta_2 (p_c, p_c^0) \frac{1}{|p_c|^{\frac{1}{2}}} \left( \frac{\sin^2(\delta_b b)}{\delta_b^2} + \gamma^2 \right) (|p_b| \{b, N\} + N \text{sgn}(p_b)) \\ & \left. + 2N \frac{\partial \beta_1 (p_b, p_b^0)}{\partial p_b} |p_c|^{\frac{1}{2}} \frac{\sin(\delta_b b)}{\delta_b} \frac{\sin(\delta_c c)}{\delta_c} \right], \end{aligned} \quad (4.26)$$

$$\begin{aligned} \dot{c} = & -\frac{1}{\gamma} \left[ \beta_1 (p_b, p_b^0) |p_c|^{\frac{1}{2}} \frac{\sin(\delta_b b)}{\delta_b} \frac{\sin(\delta_c c)}{\delta_c} \left( 2\{c, N\} + \frac{N}{p_c} \right) \right. \\ & + \beta_2 (p_c, p_c^0) \frac{|p_b|}{|p_c|^{\frac{1}{2}}} \left( \{c, N\} - \frac{N}{2p_c} \right) \left( \frac{\sin^2(\delta_b b)}{\delta_b^2} + \gamma^2 \right) + N \frac{|p_b|}{|p_c|^{\frac{1}{2}}} \frac{\partial \beta_2 (p_c, p_c^0)}{\partial p_c} \left( \frac{\sin^2(\delta_b b)}{\delta_b^2} + \gamma^2 \right) \left. \right], \end{aligned} \quad (4.27)$$

$$\begin{aligned} \dot{p}_b = & -\frac{1}{2\gamma} \left[ 2\beta_1 (p_b, p_b^0) |p_c|^{\frac{1}{2}} \frac{\sin(\delta_c c)}{\delta_c} \left( \frac{\sin(\delta_b b)}{\delta_b} \{p_b, N\} - N \cos(\delta_b b) \right) \right. \\ & \left. + \beta_2 (p_c, p_c^0) \frac{|p_b|}{|p_c|^{\frac{1}{2}}} \left( -2N \frac{\sin(\delta_b b)}{\delta_b} \cos(\delta_b b) + \left( \frac{\sin^2(\delta_b b)}{\delta_b^2} + \gamma^2 \right) \{p_b, N\} \right) \right], \end{aligned} \quad (4.28)$$

$$\begin{aligned} \dot{p}_c = & -\frac{1}{\gamma} \left[ 2\beta_1 (p_b, p_b^0) |p_c|^{\frac{1}{2}} \frac{\sin(\delta_b b)}{\delta_b} \left( \frac{\sin(\delta_c c)}{\delta_c} \{p_c, N\} - N \cos(\delta_c c) \right) \right. \\ & \left. + \beta_2 (p_c, p_c^0) \frac{|p_b|}{|p_c|^{\frac{1}{2}}} \left( \frac{\sin^2(\delta_b b)}{\delta_b^2} + \gamma^2 \right) \{p_c, N\} \right]. \end{aligned} \quad (4.29)$$

These equations will help us clarify some of the differences of our results from the previous ones, in the next sections.

## V. ISSUES RAISED BY THE NEW CORRECTIONS

As mentioned earlier, in this model, a number of differences arise due to the presence of further inverse triad corrections that we have managed to compute through the path integral method. To further highlight these differences, and also to be able to compare our results with some of the previous works, we need to specify a specific lapse  $N$ , which is needed to write the explicit equations of motion in a certain frame. One such choice takes us to the Hamiltonian in [6] in the limit of not considering these additional inverse triad quantum corrections, *i.e.* when  $\beta_1, \beta_2 \rightarrow 1$ , is

$$N^{(1)} = \frac{\gamma \delta_b p_c^{\frac{1}{2}}}{\sin(\delta_b b)}, \quad (5.1)$$

for which the effective Hamiltonian becomes

$$C_{\text{eff}}^1 = -\frac{\text{sgn}(p_c)^{\frac{1}{2}}}{2G\gamma} \left[ 2\beta_1 (p_b, p_b^0) |p_c|^{\frac{1}{2}} \frac{\sin(\delta_c c)}{\delta_c} + \beta_2 (p_c, p_c^0) |p_b| \left( \frac{\sin(\delta_b b)}{\delta_b} + \gamma^2 \frac{\delta_b}{\sin(\delta_b b)} \right) \right]. \quad (5.2)$$

It is clearly seen that this Hamiltonian matches that in [6] except for the presence of additional inverse triad corrections  $\beta_1, \beta_2$ , while they will match exactly for  $\beta_1, \beta_2 \rightarrow 1$ .

The equations of motion corresponding to this effective Hamiltonian can be derived by using the lapse (5.1) in the equations of motion (4.26)-(4.29) which yields

$$\dot{b} = -\frac{\text{sgn}(p_c)^{\frac{1}{2}}}{2} \left[ 2|p_c| \frac{\sin(\delta_c c)}{\delta_c} \frac{\partial \beta_1(p_b, p_b^0)}{\partial p_b} + \beta_2(p_c, p_c^0) \text{sgn}(p_b) \left( \frac{\sin(\delta_b b)}{\delta_b} + \gamma^2 \frac{\delta_b}{\sin(\delta_b b)} \right) \right], \quad (5.3)$$

$$\dot{c} = -\text{sgn}(p_c)^{\frac{1}{2}} \left[ 2\beta_1(p_b, p_b^0) \frac{\sin(\delta_c c)}{\delta_c} \text{sgn}(p_c) + |p_b| \frac{\partial \beta_2(p_c, p_c^0)}{\partial p_c} \left( \frac{\sin(\delta_b b)}{\delta_b} + \gamma^2 \frac{\delta_b}{\sin(\delta_b b)} \right) \right], \quad (5.4)$$

$$\dot{p}_b = \frac{\text{sgn}(p_c)^{\frac{1}{2}}}{2} \beta_2(p_c, p_c^0) |p_b| \cos(\delta_b b) \left( 1 - \gamma^2 \frac{\delta_b^2}{\sin^2(\delta_b b)} \right), \quad (5.5)$$

$$\dot{p}_c = 2\text{sgn}(p_c)^{\frac{1}{2}} \beta_1(p_b, p_b^0) |p_c| \cos(\delta_c c). \quad (5.6)$$

The lapse (5.1), however, is not the only choice for which the effective Hamiltonian will be the same as the Hamiltonian [6], in the limit  $\beta_1, \beta_2 \rightarrow 1$ . In fact any other lapse functions  $N^{(2)}$ , such that  $\lim_{\beta_1, \beta_2 \rightarrow 1} N^{(1)} = \lim_{\beta_1, \beta_2 \rightarrow 1} N^{(2)}$ , will do, for which  $N^{(2)} = \frac{\gamma \delta_b \sqrt{p_c}}{\beta_2 \sin(\delta_b b)}$  is an example.

One of the differences due to the presence of the  $\beta_1, \beta_2$  functions is related to the minimum value of  $p_c$ . In classical theory, at the horizon,  $p_c = 4G^2 M^2$ , and by approaching the singularity,  $p_b \rightarrow 0$  and  $p_c \rightarrow 0$ , and the latter plays a more crucial role as can be seen from (2.16). But, in the effective theory, due to the discreteness of the geometry, both of these functions bounce at the singularity and their minimum is related to the minimum length. In our model however, regardless of the lapse function, this minimum is different from what has been computed in previous works. To get this minimum value, we first note that

$$Q = \frac{\sin(\delta_c c)}{\delta_c} \frac{p_c}{\beta_2(p_c, p_c^0)}, \quad (5.7)$$

is a weak Dirac observable since

$$\dot{Q} = \left\{ Q, N C_{\text{S-eff}}^{(\delta_b, \delta_c)} \right\} \approx \frac{1}{\beta_2(p_c, p_c^0)} \cos(\delta_c c) \left( \frac{p_c}{\beta_2(p_c, p_c^0)} \frac{\partial \beta_2(p_c, p_c^0)}{\partial p_c} - \frac{1}{2} \right) C_{\text{S-eff}} \approx 0. \quad (5.8)$$

On the other hand we can see from (5.6) that the extremum of  $p_c$  happens for  $\cos(\delta_c c) = 0$  or  $\sin(\delta_c c) = \pm 1$ . Using this value in (5.7) will yield

$$p_{c(\min)} = Q \delta_c \beta_2(p_{c(\min)}, p_c^0), \quad (5.9)$$

where we have chosen the + sign. After solving for  $p_{c(\min)}$  and using (4.13), one finds the minimum value to be

$$p_{c(\min)} = \frac{Q \Delta^{\frac{1}{2}}}{L_0} \frac{1}{\sqrt{1 - \left( \frac{\gamma \ell_{\text{Pl}}^2}{2Q} \right)^2}}, \quad p_c > p_c^0. \quad (5.10)$$

The similar weak Dirac observable in [6] is  $Q^{\text{C-S}} = \frac{\sin(\delta_c c)}{\delta_c} p_c$ , which makes their minimum value  $p_{c(\min)}^{\text{C-S}} = Q^{\text{C-S}} \delta_c$ . From this and (5.9), we get

$$\frac{p_{c(\min)}}{\beta_2(p_{c(\min)}, p_c^0)} = p_{c(\min)}^{\text{C-S}} \frac{Q}{Q^{\text{C-S}}} \quad (5.11)$$

which after solving for  $p_{c(\min)}$  yields

$$p_{c(\min)} = \pm \left( \frac{Q}{Q^{\text{C-S}}} \right)^2 \frac{p_{c(\min)}^{\text{C-S}}}{\sqrt{\left( \frac{Q}{Q^{\text{C-S}}} \right)^2 - \left( \frac{p_c^0}{2p_{c(\min)}^{\text{C-S}}} \right)^2}}, \quad p_c > p_c^0. \quad (5.12)$$

In case  $Q$  is equal to the constant of motion in [6]  $Q^{\text{C-S}} = \gamma L_0 GM$ , we will get

$$p_{c(\min)} = \gamma GM \sqrt{\Delta} \frac{1}{\sqrt{1 - \left( \frac{\ell_{\text{Pl}}^2}{2GM L_0} \right)^2}}, \quad p_c > p_c^0. \quad (5.13)$$

This is the value of the  $p_c$  at time of the bounce, and has a pure quantum origin such that for  $G\hbar \rightarrow 0$ , one gets  $\Delta \rightarrow 0$  and thus  $p_{c(\min)} \rightarrow 0$ . Clearly this new value for minimum of  $p_c$  is different from what computed in [6] by a factor of  $\frac{1}{\sqrt{1 - \frac{1}{4} \left( \frac{\ell_{\text{Pl}}^2}{GM L_0} \right)^2}}$ , but, it depends on

the auxiliary parameter  $L_0$ . This dependence on  $L_0$  or its rescaling  $L_0 \rightarrow \xi L_0$ , shows itself in several places. Let us consider for instance a congruence of geodesic observers and their corresponding shear and expansion. Their dependence upon  $L_0$  is an undesirable effect, since the physical results should not depend on the an auxiliary variable or its rescaling. This can be traced back to the presence of the new corrections  $\beta_1$  and  $\beta_2$ . To see this in a more concrete way, we first consider the expansion  $\theta$ . For a generic lapse it can be written as

$$\theta = \frac{\dot{p}_b}{N p_b} + \frac{\dot{p}_c}{2N p_c}, \quad (5.14)$$

which for  $N = 1$  (and on constraint surface) turns out to be

$$\begin{aligned} \theta = \frac{1}{\gamma} \left\{ \beta_1(p_b, p_b^0) |p_c|^{\frac{1}{2}} \left[ \frac{\sin(\delta_c c) \cos(\delta_b b)}{p_b \delta_c} + \frac{\sin(\delta_b b) \cos(\delta_c c)}{p_c \delta_b} \right] \right. \\ \left. + \beta_2(p_c, p_c^0) \frac{\text{sgn}(p_b)}{|p_c|^{\frac{1}{2}}} \frac{\sin(\delta_b b) \cos(\delta_b b)}{\delta_b} \right\}. \end{aligned} \quad (5.15)$$

From the transformation properties of the objects involved, it can be seen that although all the combination  $\delta_b b$ ,  $\delta_c c$ ,  $p_b \delta_c$ ,  $p_c \delta_b$  in the terms above are invariant under a rescaling  $L_0 \rightarrow \xi L_0$ , the expansion  $\theta$  itself is not, precisely because the presence and noninvariance of  $\beta_1(p_b, p_b^0)$  and  $\beta_2(p_c, p_c^0)$ .

We can also compute shear  $\sigma^2$

$$\sigma^2 = \frac{1}{3} \left( -\frac{\dot{p}_b}{N p_b} + \frac{\dot{p}_c}{N p_c} \right)^2 \quad (5.16)$$

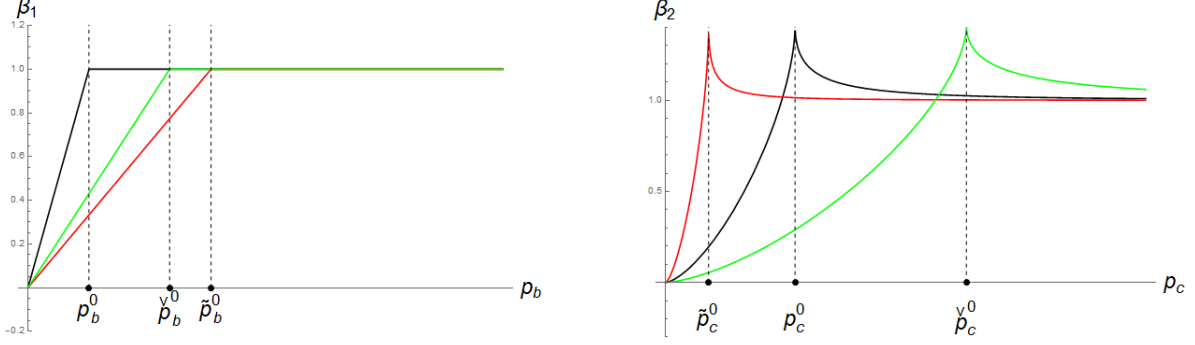


Figure 2. Comparison of the the original  $\beta_1, \beta_2$  with the new functions  $\tilde{\beta}_1, \tilde{\beta}_2$  of the first prescription and  $\check{\beta}_1, \check{\beta}_2$  of the second prescription.

to see that for  $N = 1$  we get

$$\sigma^2 = \frac{1}{3\gamma^2} \left\{ \beta_1(p_b, p_b^0) |p_c|^{\frac{1}{2}} \left[ 2 \frac{\sin(\delta_b b) \cos(\delta_c c)}{p_c \delta_b} - \frac{\sin(\delta_c c) \cos(\delta_b b)}{p_b \delta_c} \right] - \beta_2(p_c, p_c^0) \frac{\text{sgn}(p_b) \sin(\delta_b b) \cos(\delta_b b)}{|p_c|^{\frac{1}{2}} \delta_b} \right\}^2. \quad (5.17)$$

Again in the terms above, the only noninvariant parts under rescalings are  $\beta_1(p_b, p_b^0)$  and  $\beta_2(p_c, p_c^0)$ . Thus a strong hint is that a solution that renders both  $\beta_1$  and  $\beta_2$ , invariant under rescalings, will resolve all of the above issues. Finding such a solution is the subject of the next section.

## VI. PROPOSALS TO DEAL WITH THE ISSUES

These observations together with the detailed forms of  $\beta_1$  and  $\beta_2$ , suggest that some sort of interchanging  $p_b^0 \leftrightarrow p_c^0$  can fix the problem, either just in  $\beta_2$ , or in both  $\beta_1$  and  $\beta_2$ . At a first glance, it seems that this can be achieved by interchanging  $\delta_b \leftrightarrow \delta_c$ , but this has two problems: it is not clear if there are restrictions in doing so, and more importantly, although it fixes the invariance problem in  $\beta_2$ , it makes almost every other terms in  $\theta$  and  $\sigma^2$  noninvariant. So we should find a way of interchanging  $\delta_b \leftrightarrow \delta_c$  that only results in an interchange  $p_b^0 \leftrightarrow p_c^0$ , but does not lead to any modifications or interchange of  $\delta_b \leftrightarrow \delta_c$  outside  $p_b^0$  and  $p_c^0$ . In other words, it should only affect triad corrections but not the holonomy ones. By looking at (3.1), (3.6), and (3.9), we notice that this can be achieved by some sort of interchange of  $\delta_b$  and  $\delta_c$  but just in the Thiemann's formula (3.9) (which is allowed classically), and not in the computations of the curvature in (3.6). Given this observation, we make two proposals which work particularly well at or near the singularity, and are explained in the following sections.

### A. Proposal one: $\delta_b \leftrightarrow \delta_c$ in Thiemann's formula

The first proposal is to mutually interchange,  $r_0$  and  $L_0$  in  $\delta_b, \delta_c$  amounting to the exchange  $\delta_b \leftrightarrow \delta_c$  only in Thiemann's formula (3.9) which can always be done classically. This only



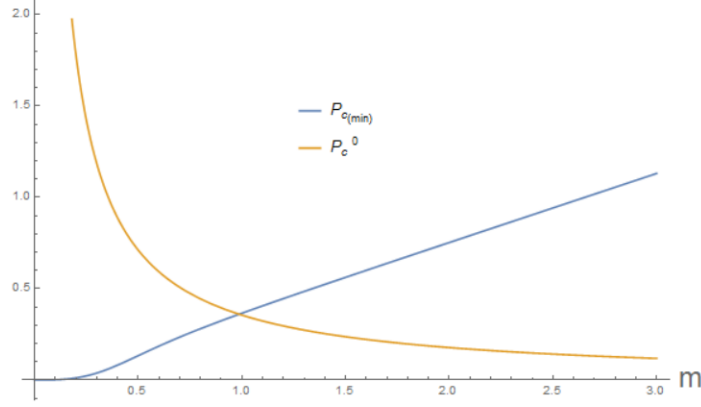


Figure 3. The effects of the corrections are relevant when  $p_{c(\min)}$  is comparable to, or smaller than  $p_c^0$ . In our proposal, this happens for  $M_B \approx M_{\text{Pl}}$ .

affects the inverse triad correction by essentially interchanging  $p_b^0 \leftrightarrow \frac{1}{2}p_c^0$ , while not altering the terms that depend on holonomy corrections. Consequently  $\delta_b$  and  $\delta_c$  remain the same whenever they appear outside  $p_b^0$  or  $p_c^0$ . As we will see, this has several desired consequences. After such an interchange  $\delta_b \leftrightarrow \delta_c$ , the quantities  $p_b^0$ ,  $p_c^0$ ,  $\beta_1$  and  $\beta_2$  are replaced by their new versions denoted by a tilde as

$$\tilde{p}_b^0 = \frac{1}{2}\gamma\ell_{\text{Pl}}^2\delta_c = \frac{1}{2}p_c^0, \quad (6.1)$$

$$\tilde{p}_c^0 = \gamma\ell_{\text{Pl}}^2\delta_b = 2p_b^0, \quad (6.2)$$

$$\tilde{\beta}_1(p_b, \tilde{p}_b^0) = \frac{|p_b + \tilde{p}_b^0| - |p_b - \tilde{p}_b^0|}{2\tilde{p}_b^0}, \quad (6.3)$$

$$\tilde{\beta}_2(p_c, \tilde{p}_c^0) = |p_c|^{\frac{1}{2}} \frac{\left(\sqrt{|p_c + \tilde{p}_c^0|} - \sqrt{|p_c - \tilde{p}_c^0|}\right)}{\tilde{p}_c^0}. \quad (6.4)$$

The profile of these new function  $\tilde{\beta}_1, \tilde{\beta}_2$  in comparison with the original  $\beta_1, \beta_2$  and the new function from the second prescription  $\check{\beta}_1, \check{\beta}_2$  (see next section) can be seen in Fig. 2. Considering (3.8), we see that under a rescaling  $L_0 \rightarrow \xi L_0$ , one gets

$$\tilde{p}_b^0 \rightarrow \tilde{p}_b^{0'} = \frac{\tilde{p}_b^0}{\xi}, \quad (6.5)$$

$$\tilde{p}_c^0 \rightarrow \tilde{p}_c^{0'} = \tilde{p}_c^0, \quad (6.6)$$

$$\tilde{\beta}_1(p_b, \tilde{p}_b^0) \rightarrow \tilde{\beta}_1'(p_b', \tilde{p}_b^{0'}) = \tilde{\beta}_1\left(p_b, \frac{\tilde{p}_b^0}{\xi^2}\right), \quad (6.7)$$

$$\tilde{\beta}_2(p_c, \tilde{p}_c^0) \rightarrow \tilde{\beta}_2'(p_c', \tilde{p}_c^{0'}) = \tilde{\beta}_2(p_c, \tilde{p}_c^0). \quad (6.8)$$

It is seen that now  $\tilde{\beta}_2$  is invariant under rescalings while  $\tilde{\beta}_1$  is not. Looking at (2.17) and (2.18) and the form of  $\tilde{\beta}$ 's, we notice that since  $\tilde{\beta}_1$  becomes important for small  $p_b$  (also see Fig. 1), it modifies the behavior near the horizon, while  $\beta_2$  is important for the modifications near the singularity because it becomes different from unity for small  $p_c$ .

However, for  $p_b < \tilde{p}_b^0$  where  $\tilde{\beta}_1$  becomes important, it will depend on the rescaling. This means that the classical behavior at the horizon will be affected in this way. But, if

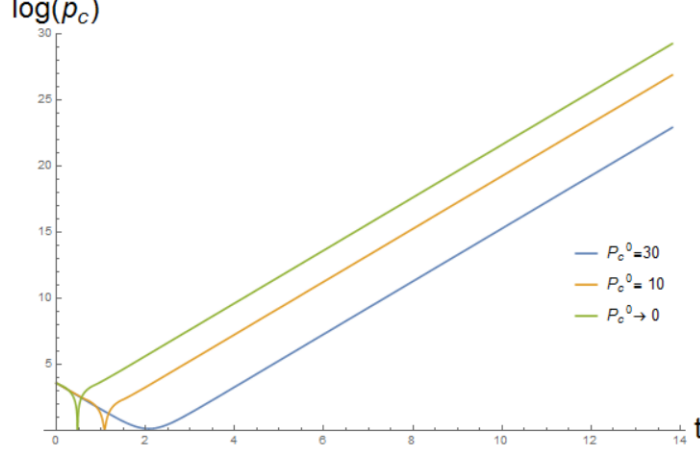


Figure 4. Effects of the inverse triad corrections on the evolution of  $p_c(t)$  for distinct values of  $p_c^0$ . The starting point of the curves corresponds to the same black hole mass, while the end of them is associated to the white hole mass. Here we have considered a black hole with mass 2 in Planck units,  $L_0 = 10$  and  $\gamma = .2375$ .

one assumes that one can consider  $L_0 \rightarrow \infty$  at the end, this modification will be avoided (because the region of  $p_b < \tilde{p}_b^0$  disappears and we only have  $p_b > 0$  for which  $\tilde{\beta}_1 \rightarrow 1$  and obviously invariant, see (6.3)). Furthermore the quantum corrections at the singularity will not be modified, since for this limit,  $\tilde{\beta}_2$  is unaffected. This limit can be taken for a genuine cosmological model and here we will assume that it is also valid for black holes.

The first nice consequence of this prescription is that the minimum value of  $p_c$  which results in singularity avoidance is now independent of  $L_0$ ,

$$p_{c(\min)} = \gamma GM \sqrt{\Delta} \frac{1}{\sqrt{1 - \left(\frac{\ell_{\text{Pl}}}{2GM}\right)^4}}, \quad p_c > \tilde{p}_c^0 \quad (6.9)$$

while still retaining the factors of modification  $\left(1 - \left(\frac{\ell_{\text{Pl}}}{2GM}\right)^4\right)^{-\frac{1}{2}}$ , which makes the minimum for the bounce larger than the previous results. As is seen from the above expression and also from Fig. 3, this effect is important when  $M \approx M_{\text{Pl}}$ . Furthermore, given this value of  $p_{c(\min)}$ , the curvature scalars are universally bounded.

Using the new tilde variables (6.1)-(6.4) to compute the expansion and shear, we get similar expression as in (5.15) and (5.17), but with replacing  $\beta_1 \rightarrow \tilde{\beta}_1$ ,  $\beta_2 \rightarrow \tilde{\beta}_2$ ,  $p_b^0 \rightarrow \tilde{p}_b^0$  and  $p_c^0 \rightarrow \tilde{p}_c^0$ . As a result, all the terms inside the expressions for  $\theta$  and  $\sigma^2$ , that are proportional to  $\tilde{\beta}_2$ , not only become independent of  $L_0$ , but also become invariant under its rescalings. On the other hand, the terms proportional to  $\tilde{\beta}_1$ , are not invariant under its rescalings. However, with our assumption  $L_0 \rightarrow \infty$  for which  $\tilde{\beta}_1 \rightarrow 1$ , the latter issue is bypassed. Furthermore, the values of  $\theta$  and  $\sigma^2$  for  $N = 1$  now remain finite at both the singularity and the horizon, given that at the horizon,  $\tilde{\beta}_1 \rightarrow 0$ , and  $\tilde{\beta}_2$  is finite but nonzero, and at the singularity  $\tilde{\beta}_1, \tilde{\beta}_2 \rightarrow 0$ . In addition, with  $L_0 \rightarrow \infty$ , they are both invariant.

Another observation is about the mass of the white hole. The behavior of  $p_c$  in time, depends on the size of the parameter  $\tilde{p}_c^0$ , and particularly, as can be seen from Fig. 4, the larger the size of  $\tilde{p}_c^0$ , the larger the later values of  $p_c$ . The mass of the black hole and white

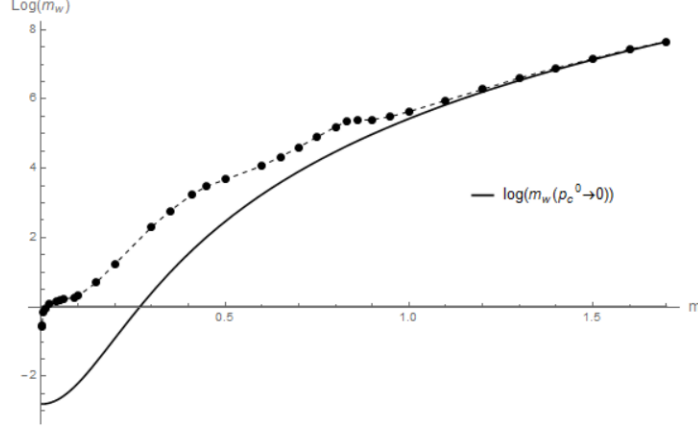


Figure 5. Comparing the behavior of  $M_W (M_B)$  without inverse triad corrections (solid line) and the case with  $\tilde{\beta}_2$  corrections.

hole are

$$M_B = M = \frac{\sqrt{p_c(t_i)}}{2G}, \quad M_W = \frac{\sqrt{p_c(t_f)}}{2G}, \quad (6.10)$$

in which  $t_i$  and  $t_f$  are the initial and final times when black hole forms, and then when after bouncing back to the new white hole with its own Schwarzschild radius, respectively. Here we have used  $p_c = r_{\text{Schw}}^2$  with  $r_{\text{Schw}}$  being the Schwarzschild radius of the black and white holes at these two moments in time. As can be seen from Fig. 4,  $M_W$  then depends on the value of  $\tilde{p}_c^0$  and thus on  $\tilde{\beta}_2$ . It turns out then that  $M_W(\beta_2 \neq 1) > M_W(\beta_2 \rightarrow 1)$ . The effect of new correction on the relation between the black hole and white hole masses can be seen from the graph of  $M_W (M_B)$  in Fig. 5.

### B. Proposal two: $\delta_b \leftrightarrow 1/\delta_c$ in Thiemann's formula

The second proposal is to mutually interchange  $\delta_b \leftrightarrow \frac{1}{\delta_c}$ , restricted again to the Thiemann's formula (3.9). This leads to the quantities  $p_b^0, p_c^0, \beta_1$  and  $\beta_2$  being replaced by their new versions denoted by  $\check{\cdot}$  as

$$\check{p}_b^0 = \frac{1}{2} \frac{\gamma \ell_{\text{Pl}}^2}{\delta_c} = \frac{1}{2} \frac{\gamma^2 \ell_{\text{Pl}}^4}{p_c^0}, \quad (6.11)$$

$$\check{p}_c^0 = \frac{\gamma \ell_{\text{Pl}}^2}{\delta_b} = \frac{1}{2} \frac{\gamma^2 \ell_{\text{Pl}}^4}{p_b^0}, \quad (6.12)$$

$$\check{\beta}_1(p_b, \check{p}_b^0) = \frac{|p_b + \check{p}_b^0| - |p_b - \check{p}_b^0|}{2\check{p}_b^0}, \quad (6.13)$$

$$\check{\beta}_2(p_c, \check{p}_c^0) = |p_c|^{\frac{1}{2}} \frac{\left( \sqrt{|p_c + \check{p}_c^0|} - \sqrt{|p_c - \check{p}_c^0|} \right)}{\check{p}_c^0}. \quad (6.14)$$

In Fig. 2, the behavior of these new  $\check{\beta}_1, \check{\beta}_2$  functions is compared to the original functions, and the functions from the first prescription. Interestingly, now both  $\check{\beta}_1, \check{\beta}_2$  are invariant under rescalings. Thus, the effective behavior is independent of the auxiliary rescalings both

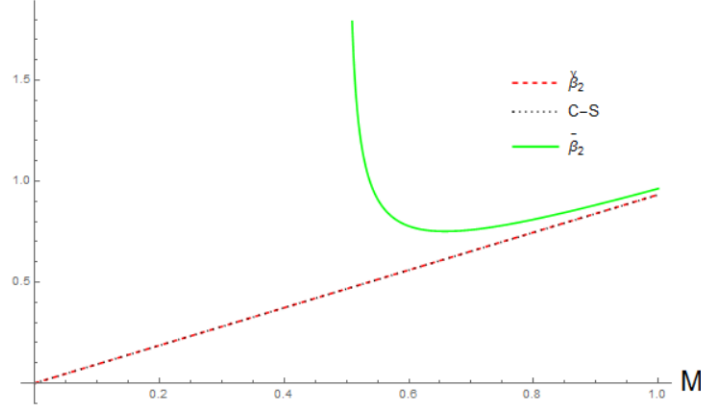


Figure 6. Dependence of  $p_{c(\min)}$  on black hole mass  $M$ . The case without corrections denoted by C-S, is compared to the two prescriptions labeled by their corresponding  $\beta_2$  functions. Although the lines for the second prescription and no-correction cases look the same, they have different slopes due to the modification factor  $\left(1 - \left(\frac{\ell_{\text{Pl}}^2}{\Delta}\right)^2\right)^{-\frac{1}{2}}$  of the former case.

on the horizon and at the singularity, and thus there is no need for the additional assumption  $L_0 \rightarrow \infty$ .

Let us see the effect of these prescription on  $p_{c(\min)}$ . Here again, a nice consequence of the prescription is that the minimum value of  $p_c$  is independent of  $L_0$ ,

$$p_{c(\min)} = \gamma G M \sqrt{\Delta} \frac{1}{\sqrt{1 - \left(\frac{\ell_{\text{Pl}}^2}{\Delta}\right)^2}}, \quad p_c > \check{p}_c^0. \quad (6.15)$$

Compared to the previous works, this is now modified by a factor  $\left(1 - \left(\frac{\ell_{\text{Pl}}^2}{\Delta}\right)^2\right)^{-\frac{1}{2}}$ , and unlike proposal one, this factor is now independent of the black hole mass, and instead depends on the ratio of the Planck area to the minimum area. These modifications are rather large for any black hole regardless of the mass. In any case, this value of  $p_{c(\min)}$ , means that in this case too, the curvature scalars are universally bounded. It is worth noting that, in this case, as expected,  $p_{c(\min)} \rightarrow 0$  if  $\Delta \rightarrow 0$ , which is the case for a theory with a continuous spacetime. Fig. 6 compares the dependence of  $p_{c(\min)}$  on black hole mass,  $M$ , for the two prescriptions as well as the case without the corrections.

The shear  $\sigma^2$  and expansion  $\theta$  have similar expression as in (5.15) and (5.17), but with replacing  $\beta_1 \rightarrow \check{\beta}_1$ ,  $\beta_2 \rightarrow \check{\beta}_2$ ,  $p_b^0 \rightarrow \check{p}_b^0$  and  $p_c^0 \rightarrow \check{p}_c^0$ . Given that  $\check{\beta}_1$  and  $\check{\beta}_2$  are both invariant under rescalings, both  $\theta$  and  $\sigma^2$  are now fully invariant too, without the need for any further assumptions. Finally they both remain finite on both horizon and at the classical singularity since at the horizon,  $\check{\beta}_1 \rightarrow 0$ , and  $\check{\beta}_2$  is finite but nonzero, and at the singularity  $\check{\beta}_1, \check{\beta}_2 \rightarrow 0$ .

Finally, the numerical evolution of  $p_c$  in time for the case without correction is compared to the second prescription in Fig. 7. It is seen that there is a horizontal asymptote corresponding to the case of second prescription, which gives a final value for the  $p_c$  which is smaller than the final value without corrections. In the case with no corrections, *i.e.*, in [6], the evolution of  $p_c$  stops at a finite time and the corresponding  $p_c$  is interpreted as the position of the horizon (the large dot in Fig. 7). In the presence of corrections and using

the second proposal, however,  $p_c$  has an asymptotic behavior that depends on  $p_b^0$ . Thus this asymptotic value may be interpreted as the horizon, although it is not reached at a finite time.

## VII. DISCUSSION

The quest for a quantum theory of gravity involves looking for physical imprints of the merging of quantum and gravity effects in systems like black holes that classically exhibit singularities according to general relativity. In the case of Schwarzschild black hole, loop quantum gravity predicts the resolution of the classical singularity as well as a bouncing scenario connecting the black hole to a white hole, a phenomenon also predicted for some cosmological models, in such a case connecting a contracting with an expanding phase of the Cosmos. Previous research on the loop quantized black hole interior, either purely quantum [3] or effective [4–6, 14, 27, 28], shares this feature. However more insight has been obtained with the latter in that it allowed to investigate the physical independence from auxiliary parameters required in the formulation of the theory to further improve the description of the black to white hole bounce. Yet, all these works ignore the effects of the inverse triad corrections that enter the Hamiltonian constraint, basically to simplify the analysis.

In this work, we have extended and built up over the previous important works about the effective theory of the interior of the Schwarzschild modeled as a Kantowski-Sachs spacetime bouncing and with a resolved singularity. We started by using the proposal for the fiducial cell parameters in [6] to cope with the noncompact topology  $\mathbb{R} \times \mathbb{S}^2$  of the model, and used a polymer path integral approach as systematic way to derive an effective Hamiltonian which automatically incorporates the inverse triad corrections. The effective Hamiltonian without these corrections resembles exactly the one in previous works. Although the inclusion of these corrections sheds more light on the physical nature of the problem, it raises some well-known issues in the analysis if one makes the usual choice of the parameters entering the model  $\delta_b, \delta_c$  in both curvature sector as well as in the inverse triad sector [6]. Such issues were the main reason they have been mostly ignored in previous works. These issues include the dependence of physical quantities like the expansion and shear on the rescaling of the fiducial parameter that is used to define the fiducial cell. Introduction of this cell is necessary to be able to compute the symplectic structure. In this case, the cell is a three dimensional cylinder whose height  $L_0$  is the fiducial parameter, while its base is identified with a physical parameter, namely, the classical Schwarzschild radius. Furthermore, although the “minimum radius of black hole at bounce”,  $p_{c(\min)}$ , that we obtain here is different from the previous works, it also depends on the fiducial parameter  $L_0$  and its rescalings, which thus renders the model physically unacceptable.

We tackle these issues by exploring the source of the dependence on the auxiliary parameters. It turns out that triad corrections, contained into two function  $\beta_1$  and  $\beta_2$ , are both noninvariant under their rescalings. The first function  $\beta_1$  is important for the behavior of the black hole at the horizon, while the second one,  $\beta_2$ , is important for the behavior at or near the singularity. Looking more closely into the form of these correction functions, we see that some sort of interchanging of the parameters  $\delta_b$  and  $\delta_c$ , might resolve the issue; recall these are used in the representation of the inverse triads in Thiemann’s formula, as well as in computing the curvatures. Further inspection reveals that if one only interchanges the parameters  $\delta_b$  and  $\delta_c$  in Thiemann’s formula, one could make  $\beta_1$  and  $\beta_2$  invariant, and furthermore, nothing in the computation of the curvature changes. In other words only the

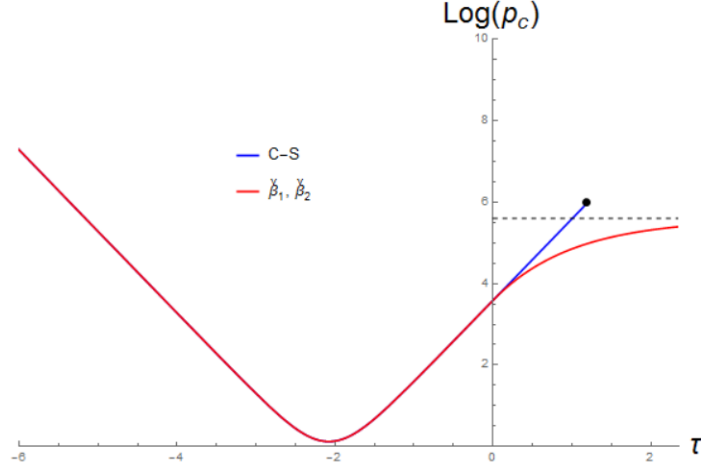


Figure 7. The evolution of  $p_c$  for the case without corrections denoted by C-S, versus the second prescriptions labeled by its corresponding  $\check{\beta}_2$  functions. Note that the latter case has an asymptote.

terms inside  $\beta_1$  and  $\beta_2$  are affected, which is the effect we are looking for.

Given this insight, we study two proposals. The first one consists of an interchange  $\delta_b \leftrightarrow \delta_c$ . As a first result, the minimum “radius” at the bounce  $p_{c(\min)}$ , now becomes independent of the auxiliary parameter and is modified because of the presence of the new corrections, such that its value is now larger than the value computed in previous works. This modification is particularly important when the mass of the black hole is comparable to the Planck’s mass. Furthermore, the function  $\beta_2$  also becomes invariant. To investigate this case further, we consider a congruence of geodesic observers and show that the terms in the corresponding expansion  $\theta$  and shear  $\sigma^2$  proportional to  $\beta_2$  are now also invariant. However, in this proposal,  $\beta_1$  remains noninvariant. But the issues that correspond to this function not being invariant can be bypassed by assuming that at the end, one can take the limit  $L_0 \rightarrow \infty$  which may be interpreted as the black hole being eternal. This limit is legitimate in cosmology but in a black hole setting, we should be more careful about its consequences. Using this limit,  $\theta$  and  $\sigma^2$  become both completely invariant under rescalings. This state of affairs can be improved as we next discuss it.

The second proposal amounts to the interchange  $\delta_b \leftrightarrow 1/\delta_c$  in the original choice. It turns out in this case both  $\beta_1$  and  $\beta_2$  are invariant under rescalings without any need for additional assumptions such as  $L_0 \rightarrow \infty$ . As for the congruence of geodesic observers, both expansion  $\theta$  and shear  $\sigma^2$  now become fully (and not partially) invariant. Another new result with this proposal is that not only the minimum “radius” at the bounce  $p_{c(\min)}$  is different, but now it does not depend on the mass of the black hole, but rather depends on the ratio of the minimum area to the Planck area, and is universal for all masses. This, in general, is certainly larger than what we derived from the previous proposal, particularly in cases where the mass of the black hole is much larger than the Planck’s mass.

Finally, we notice that the issue of mismatch between the masses of initial black hole  $M_B$ , and the final white hole  $M_W$ , worsens by introducing these new corrections such that  $M_W(\beta_2 \neq 1) > M_W(\beta_2 \rightarrow 1)$ . As mentioned before, this is due to the anisotropic nature of the Kantowski-Sachs model.

Our results open the door to incorporating further quantum inverse triad corrections in other black hole models, as well as in other quantum gravitational systems, and provides a

method to deal with the issues raised by them, which is the reason they are mostly ignored in previous works. Hence, we believe that it is important to continue investigating similar gravitational models using this path integral approach. In particular, it would be interesting to combine our method with that of [26] to further explore the black-to-white hole mass mismatch problem as well as to include the inverse triad corrections in some recent works [27, 28].

## ACKNOWLEDGMENTS

The authors would like to acknowledge the support from the CONACyT Grant No. 237351. S.R. would like to thank the CONACyT SNI support 59344. J.C.R. acknowledges the support of the grant from UAM-I. H.A.M.T. acknowledges the kind hospitality of the Physics department of the ESFM, IPN, during his sabbatical year

- 
- [1] Thomas Thiemann, *Modern Canonical Quantum General Relativity*, Cambridge Monographs on Mathematical Physics (Cambridge University Press, 2007).
  - [2] Carlo Rovelli, *Quantum gravity*, Cambridge Monographs on Mathematical Physics (Univ. Pr., Cambridge, UK, 2004).
  - [3] Abhay Ashtekar and Martin Bojowald, “Quantum geometry and the Schwarzschild singularity,” *Class. Quant. Grav.* **23**, 391–411 (2006), arXiv:gr-qc/0509075 [gr-qc].
  - [4] Christian G. Boehmer and Kevin Vandersloot, “Stability of the Schwarzschild Interior in Loop Quantum Gravity,” *Phys. Rev.* **D78**, 067501 (2008), arXiv:0807.3042 [gr-qc].
  - [5] Leonardo Modesto, “Loop quantum black hole,” *Class. Quant. Grav.* **23**, 5587–5602 (2006), arXiv:gr-qc/0509078 [gr-qc].
  - [6] Alejandro Corichi and Parampreet Singh, “Loop quantization of the schwarzschild interior revisited,” *Class. Quant. Grav.* **33**, 055006 (2016), 1506.08015.
  - [7] Daniel Cartin and Gaurav Khanna, “Wave functions for the Schwarzschild black hole interior,” *Phys. Rev.* **D73**, 104009 (2006), arXiv:gr-qc/0602025 [gr-qc].
  - [8] Rodolfo Gambini, Jorge Pullin, and Saeed Rastgoo, “New variables for 1+1 dimensional gravity,” *Class. Quant. Grav.* **27**, 025002 (2010), arXiv:0909.0459 [gr-qc].
  - [9] Saeed Rastgoo, “A local true Hamiltonian for the CGHS model in new variables,” (2013), arXiv:1304.7836 [gr-qc].
  - [10] Alejandro Corichi, Asieh Karami, Saeed Rastgoo, and Tatjana Vukašinac, “Constraint Lie algebra and local physical Hamiltonian for a generic 2D dilatonic model,” *Class. Quant. Grav.* **33**, 035011 (2016), arXiv:1508.03036 [gr-qc].
  - [11] Alejandro Corichi, Javier Olmedo, and Saeed Rastgoo, “Callan-Giddings-Harvey-Strominger vacuum in loop quantum gravity and singularity resolution,” *Phys. Rev.* **D94**, 084050 (2016), arXiv:1608.06246 [gr-qc].
  - [12] Rodolfo Gambini, Jorge Pullin, and Saeed Rastgoo, “Quantum scalar field in quantum gravity: The vacuum in the spherically symmetric case,” *Class. Quant. Grav.* **26**, 215011 (2009), arXiv:0906.1774 [gr-qc].
  - [13] Rodolfo Gambini, Javier Olmedo, and Jorge Pullin, “Quantum black holes in Loop Quantum Gravity,” *Class. Quant. Grav.* **31**, 095009 (2014), arXiv:1310.5996 [gr-qc].

- [14] Jerónimo Cortez, William Cuervo, Hugo A. Morales-Técotl, and Juan C. Ruelas, “Effective loop quantum geometry of Schwarzschild interior,” *Phys. Rev.* **D95**, 064041 (2017), arXiv:1704.03362 [gr-qc].
- [15] Rosa Doran, Francisco S. N. Lobo, and Paulo Crawford, “Interior of a Schwarzschild black hole revisited,” *Found. Phys.* **38**, 160–187 (2008), arXiv:gr-qc/0609042 [gr-qc].
- [16] Abhay Ashtekar, Stephen Fairhurst, and Joshua L. Willis, “Quantum gravity, shadow states, and quantum mechanics,” *Class. Quant. Grav.* **20**, 1031–1062 (2003), arXiv:gr-qc/0207106 [gr-qc].
- [17] Hugo A. Morales-Técotl, Daniel H. Orozco-Borunda, and Saeed Rastgoo, “Polymer quantization and the saddle point approximation of partition functions,” *Phys. Rev.* **D92**, 104029 (2015), arXiv:1507.08651 [gr-qc].
- [18] Hugo A. Morales-Técotl, Daniel H. Orozco-Borunda, and Saeed Rastgoo, “Polymerization, the Problem of Access to the Saddle Point Approximation, and Thermodynamics,” in *Proceedings, 14th Marcel Grossmann Meeting*, Vol. 4 (2017) pp. 4054–4059, arXiv:1603.08076 [gr-qc].
- [19] Hugo A. Morales-Técotl, Saeed Rastgoo, and Juan C. Ruelas, “Path integral polymer propagator of relativistic and nonrelativistic particles,” *Phys. Rev.* **D95**, 065026 (2017), arXiv:1608.04498 [gr-qc].
- [20] Abhay Ashtekar and Parampreet Singh, “Loop Quantum Cosmology: A Status Report,” *Class. Quant. Grav.* **28**, 213001 (2011), arXiv:1108.0893 [gr-qc].
- [21] Abhay Ashtekar, Martin Bojowald, and Jerzy Lewandowski, “Mathematical structure of loop quantum cosmology,” *Adv. Theor. Math. Phys.* **7**, 233–268 (2003), arXiv:gr-qc/0304074 [gr-qc].
- [22] Abhay Ashtekar, Tomasz Pawłowski, and Parampreet Singh, “Quantum Nature of the Big Bang: An Analytical and Numerical Investigation. I.” *Phys. Rev.* **D73**, 124038 (2006), arXiv:gr-qc/0604013 [gr-qc].
- [23] Abhay Ashtekar, Tomasz Pawłowski, and Parampreet Singh, “Quantum nature of the big bang: Improved dynamics,” *Phys. Rev.* **D74**, 084003 (2006), gr-qc/0607039.
- [24] Jibril Ben Achour, Frédéric Lamy, Hongguang Liu, and Karim Noui, “Polymer Schwarzschild black hole: An effective metric,” *EPL* **123**, 20006 (2018), arXiv:1803.01152 [gr-qc].
- [25] Martin Bojowald, Suddhasattwa Brahma, and Dong-han Yeom, “Effective line elements and black-hole models in canonical loop quantum gravity,” *Phys. Rev.* **D98**, 046015 (2018), arXiv:1803.01119 [gr-qc].
- [26] Javier Olmedo, Sahil Saini, and Parampreet Singh, “From black holes to white holes: a quantum gravitational, symmetric bounce,” *Class. Quant. Grav.* **34**, 225011 (2017), arXiv:1707.07333 [gr-qc].
- [27] Abhay Ashtekar, Javier Olmedo, and Parampreet Singh, “Quantum Transfiguration of Kruskal Black Holes,” *Phys. Rev. Lett.* **121**, 241301 (2018), arXiv:1806.00648 [gr-qc].
- [28] Abhay Ashtekar, Javier Olmedo, and Parampreet Singh, “Quantum extension of the Kruskal spacetime,” *Phys. Rev.* **D98**, 126003 (2018), arXiv:1806.02406 [gr-qc].
- [29] Abhay Ashtekar, Miguel Campiglia, and Adam Henderson, “Path Integrals and the WKB approximation in Loop Quantum Cosmology,” *Phys. Rev.* **D82**, 124043 (2010), arXiv:1011.1024 [gr-qc].